Terahertz conductivity and ultrafast dynamics of photoinduced charge carriers in intrinsic 3C and 6H silicon carbide

Andrea Rubano,[1,2,a] Martin Wolf,[1] and Tobias Kampfrath[1]
[1] *Fritz Haber Institute of the Max Planck Society, Faradayweg 4-6, 14195 Berlin, Germany.*
[2] *Dipartimento di Fisica, Università di Napoli Federico II, and Istituto SPIN-CNR, Via Cintia, 80100 Napoli, Italy.*

(Dated: 22 May 2014)

The terahertz conductivity of photoinduced charge carriers in two common polytypes of silicon carbide, 3C-SiC and 6H-SiC, is studied on picosecond timescales using an optical-pump / THz-probe technique. We find that the conductivity, measured from 0.7 to 3 THz, is well described by the Drude model, and obtain a velocity relaxation time of 75 fs, independent of sample and charge-carrier density. In contrast, the carrier relaxation rates in the two polytypes differ by orders of magnitude: in 6H- and 3C-SiC, recombination proceeds on a time scale of few picoseconds and beyond nanoseconds, respectively.

The technological demand for high-power, high-temperature, and high-field electronic devices requires robust base materials.[1] In this respect, silicon carbide (SiC) is one of the most promising candidates owing to its excellent electrical and structural properties. SiC exists in a large number of polytypes that can be all thought of resulting from stacking three types of bilayer structures (A, B and C) in a certain periodic sequence. The most commonly encountered polytypes are 3C-SiC (stacking order ABC) and 6H-SiC (ABCACB), resulting in a zincblende (two atoms per unit cell) and hexagonal structure (twelve atoms per unit cell), respectively.[2] At room temperature, 3C- and 6H-SiC have an an indirect electronic energy gap of 2.36 eV and 3.0 eV, respectively.[2]

SiC exhibits exceptional properties that are to a large extent related to the Si-C bond, leading to a stronger localization of the charge density and a larger band gap compared to Si.[2,3] For example, the thermal conductivity of 4.9 and 5.0 W/cm K and breakdown electric field of 3.2 and 1.5 MV/cm for 6H-SiC and 3C-SiC, respectively,[4,5] are about 3 to 5 times larger than those of Si.[2] In addition, the various polytypes make SiC an interesting host material for controlling single electron spins.[6] Also, 6H-SiC may serve as suitable starting material for large-scale graphene production.[7]

In order to improve the quality and performance of SiC-based devices, knowledge of fundamental parameters such as the mobility of charge carriers is crucial. Moreover, charge transport is also of considerable interest from the perspective of fundamental physics. So far, the carrier mobility has not been measured in the case of intrinsic samples since they are wide band-gap insulators. A possible approach is to create a transient free-carrier population, for instance by exciting the material with a light pulse. The optical generation of charge carriers circumvents complications arising from chemical doping and, in addition, provides the opportunity to measure out-of-equilibrium parameters.

So far, the dynamics of photoinduced charge carriers in intrinsic 3C- and 6H-SiC has been studied using pump-probe experiments[8–10], however, with a time resolution of nanoseconds and at optical probe frequencies, far above the charge-carrier scattering rates that usually lye in the terahertz (THz) frequency range.[12] Deeper insight could be obtained by performing conductivity measurements using THz electromagnetic pulses having picosecond duration. From such broadband THz conductivity spectra, parameters such as carrier density and velocity relaxation rate can be inferred directly, without using electrical contacts which are often problematic with insulators.[14]

In this Letter, we apply optical-pump / THz-probe spectroscopy to intrinsic 3C- and 6H-SiC crystals and determine the transient conductivity of the photoinduced charge carriers in the range from 0.7 to 3 THz in a contact-free manner. Analyzing the THz conductivity spectra by means of the Drude model, we are able to extract transient carrier density and velocity relaxation rate. The values found are in good agreement with mobility values found in doped samples using static transport measurements. However, while the velocity relaxation rate is similar in the two polytype samples, we find very different charge-carrier relaxation dynamics.

In our experiment, we study intrinsic[15] double-side-polished 3C-SiC(100) and 6H-SiC(0001) single crystals with a thickness of 140 μm and 180 μm, respectively. To determine their conductivity in a contactless manner, we measure the sample transmittance with respect to THz electromagnetic radiation. For this purpose, THz pulses are generated by optical rectification[13] of femtosecond laser pulses (energy of 1 mJ, center wavelength of 800 nm, duration of 40 fs, repetition rate of 1 kHz) in a ZnTe(110) crystal (thickness of 0.5 mm, aperture of 10 mm). After traversal of the SiC sample crystal, the transient electric field of the THz pulses is detected by electrooptic sampling in the time domain using another ZnTe(110) crystal (thickness of 0.3 mm).[12] In order to generate charge carriers prior to THz probing, the sample is excited by an optical pump pulse ($\leq$ 1 mJ, 800 nm, 40 fs, 500 Hz) un-

[a] Electronic mail: rubano@fisica.unina.it

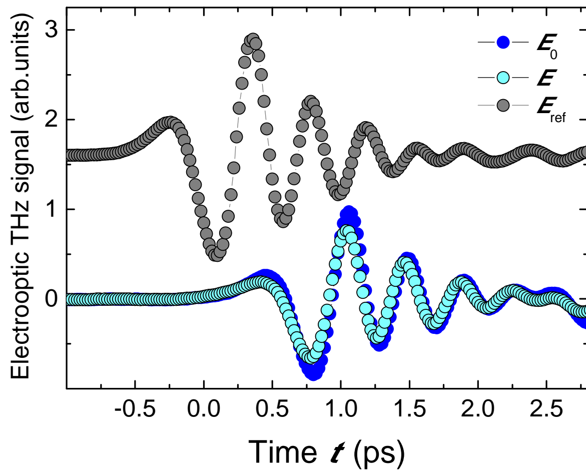

FIG. 1. Raw data of the optical-pump/THz-probe experiment. The three waveforms represent the time-domain electrooptic signals of THz electric-field pulses without sample (reference E_{ref}), after propagation through an equilibrium 6H-SiC crystal (E_0) and the sample crystal 20 ps after excitation by the pump pulse (E). Note the amplitude reduction and phase shift of E with respect to E_0.

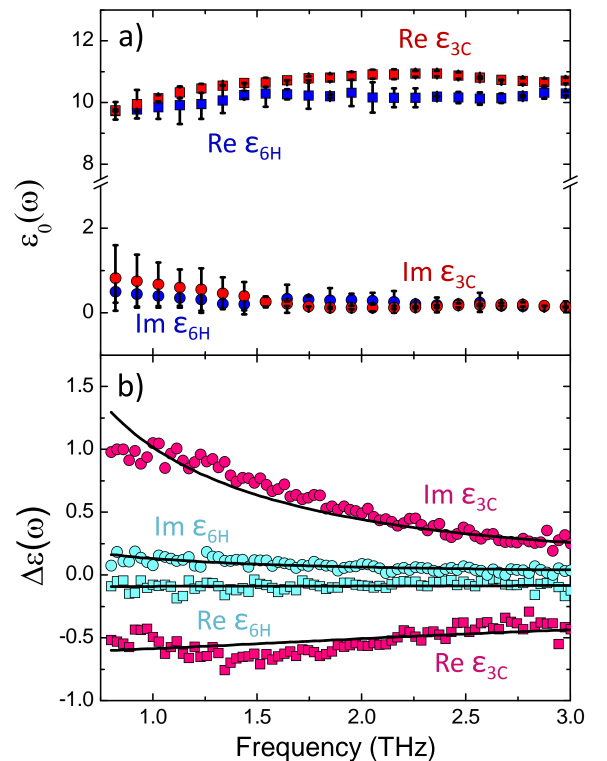

FIG. 2. Dielectric function of 3C- and 6H-SiC samples versus frequency $\omega/2\pi$, as extracted from THz raw data (Fig. 1). (a) Dielectric function ε_0 of samples in equilibrium. Error bars indicate a confidence interval of three standard deviations obtained from multiple measurements. (b) Pump-induced changes $\Delta\varepsilon$ at 20 ps after sample excitation with an intense femtosecond laser pulse. The increased absorption (positive Im $\Delta\varepsilon$) and negative Re $\Delta\varepsilon$ are indicative of transient free charge carriers. Solid lines are fits using the Drude formula [see Eq. (1) and text].

der an angle of incidence of 10° with respect to the surface normal. In order to probe a homogeneously excited sample volume, the pump-spot diameter on the sample surface was set to about 3 mm, about three times larger than the THz probe spot. In addition, the pump photon energy of 1.55 eV and the band-gap energy of 3C- and 6H-SiC imply that electron-hole pairs are generated through two-photon absorption. Measurements of incident, reflected and transmitted pump power indicate that less than 0.5 % of the incident pump pulse energy are absorbed. The delay between pump and probe pulse is varied by a translation stage. All measurements are performed at room temperature in a dry N_2 atmosphere.

Figure 1 displays three examples of THz waveforms acquired in our experiment. These signals versus time t correspond to the THz electric field impinging on the electrooptic detector, convoluted with the (relatively flat) detector response function. Thus, the waveforms roughly represent the transient electric field. While the reference signal $E_{\mathrm{ref}}(t)$ is obtained without sample, $E_0(t)$ derives from a pulse having traversed the unpumped 6H-SiC crystal. The temporal offset with respect to $E_{\mathrm{ref}}(t)$ reflects the additional time it takes the THz pulse to propagate through the sample. Finally, $E(t)$ results from a pulse that has traversed the 6H-SiC at 20 ps after excitation by the pump pulse. An amplitude reduction and a slight shift toward earlier times with respect to the unexcited specimen are apparent. This behavior indicates additional absorption and a reduction of the sample refractive index, a hallmark of the presence of free charge carriers.[12,14]

To gain more sample-intrinsic information, we apply a Fourier transformation to the time-domain waveforms of Fig. 1. By numerically inverting Fresnel formulas, we extract the complex-valued dielectric function $\varepsilon(\omega)$ (whose information content equals that of the conductivity or refractive index) over a wide range of frequencies from $\omega/2\pi = 0.7$ to 3 THz.[12,14] The result of this procedure is shown in Fig. 2(a) which displays the dielectric function $\varepsilon_0(\omega)$ for both SiC samples. While 3C-SiC is optically isotropic and exhibits a scalar ε, 6H-SiC is characterized by a dielectric tensor with components along its c axis and the plane perpendicular to it, i.e. the basal plane. However, since the THz pulse is normally incident, we only probe ε in the basal plane. As seen in Fig. 2, the frequency dependence of ε_0 is quite flat and featureless, in good agreement with earlier reports.[18] Optical phonon resonances (at about 9 THz in 6H-SiC and 24 THz for 3C-SiC)[16,17] are well above the investigated spectral range, and no other low-energy resonances are observed. Therefore, the refractive index $n = \sqrt{\varepsilon_0}$ of the material can be considered to be approximately constant in the investi-

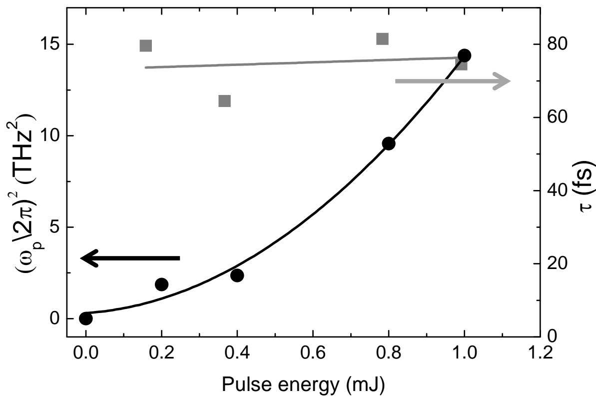

FIG. 3. Extracted squared plasma frequency ω_p^2 (black circles, left scale) and Drude scattering time τ (gray squares, right scale) as a function of pump-pulse energy for 6H-SiC. The black solid line is a parabolic fit with minimum at the origin whereas the gray solid line is a linear fit whose slope is consistent with zero. These curves show that carrier generation is dominated by two-photon absorption whereas carrier-carrier collisions make a negligible contribution to the scattering time observed.

gated spectral range. By spectral averaging, we obtain a mean value of $n \approx 3.30+0.08\mathrm{i}$ and $3.17+0.03\mathrm{i}$ for 3C-SiC and 6H-SiC, respectively.

The pump-induced changes $\Delta\varepsilon = \varepsilon - \varepsilon_0$ in the dielectric function are shown in Fig. 2(b) at 20 ps after sample excitation. The imaginary part $\mathrm{Im}\,\Delta\varepsilon$ is positive and indicates increased THz absorption, whereas the real part $\mathrm{Re}\,\Delta\varepsilon$ is negative. In addition, the absolute magnitude of both $\mathrm{Re}\,\Delta\varepsilon$ and $\mathrm{Im}\,\Delta\varepsilon$ increases toward lower frequencies. This behavior is indicative of free-carrier absorption[12,14] whose frequency dependence is often well described by the Drude formula,

$$\Delta\varepsilon = -\frac{\omega_\mathrm{p}^2}{\omega^2 + \mathrm{i}\omega/\tau}. \tag{1}$$

Here, τ is the velocity relaxation time of the carriers and

$$\omega_\mathrm{p}^2 = \frac{e^2 c Z_0 N}{m^*} \tag{2}$$

is their squared plasma frequency determined by the free-carrier density N and effective carrier mass m^*. The symbols e, c and $Z_0 \approx 377\,\Omega$ denote elementary charge, vacuum light velocity and free-space impedance, respectively. By fitting Eq. (1) to our experimental data, we achieve good agreement as seen from the solid lines in Fig. 2(b). This procedure is applied to data over a wide range of pump-probe delays and pump fluences.

The extracted values of the fit parameters ω_p and τ at 20 ps after sample excitation are plotted in Fig. 3 as a function of the pump-pulse energy for 6H-SiC. The squared plasma frequency ω_p^2 and, thus, charge-carrier density N [Eq. (2)] are found to increase quadratically with the pump fluence (black solid parabola in Fig. 3). This observation confirms that the charge carriers are induced by two-photon absorption, as expected for 800 nm excitation. In order to estimate the pump-induced carrier density N, Eq. (2) requires knowledge of the effective masses of electrons and holes along the direction of the probing THz electric field. Within the sample plane, the reported values are[19,20] $m_\mathrm{h}^{6\mathrm{H}} = 0.66 m_\mathrm{e}$, $m_\mathrm{e}^{6\mathrm{H}} = 0.48 m_\mathrm{e}$, $m_\mathrm{h}^{3\mathrm{C}} = 0.48 m_\mathrm{e}$ and $m_\mathrm{e}^{3\mathrm{C}} = 0.25 m_\mathrm{e}$ where m_e is the free electron mass. These values indicate that in both SiC polytypes, the lighter electrons contribute to the conductivity more than holes. Since the number of electrons and holes is the same, we utilize the averages $m^{6\mathrm{H}} = 0.57 m_\mathrm{e}$ and $m^{3\mathrm{C}} = 0.36 m_\mathrm{e}$. Using these values, and Eq. (2), we estimate $N \approx 2 \times 10^{16}$ cm^{-3} (6H) and $N \approx 1.5 \times 10^{16}$ cm^{-3} (3C) at a pump-pulse energy of 1 mJ. These values are consistent with a rough estimate of the pump pulse energy absorbed in the samples (see above).

As seen in Fig. 3, the Drude scattering time τ as a function of the pump-pulse energy can be represented by a linear fit curve with a slope 4 times smaller than its standard deviation, thus τ does not change upon varying the density of photoinduced charge carriers over the investigated range. We conclude that τ is predominantly determined by carrier-phonon and carrier-impurity scattering rather than carrier-carrier scattering, which is expected to become dominant at higher excitation densities. Our fits [Fig. 2(b)] yield scattering times of $\tau = (75 \pm 6)$ fs for 3C-SiC and $\tau = (75 \pm 3)$ fs for 6H-SiC. These values are comparable to those found for high-quality intrinsic semiconductors such as Si ($\tau = 73$ fs)[21]. We estimate the value of the carrier mobility μ in the basal plane using the relation

$$\mu = \frac{e\tau}{m^*} \tag{3}$$

and obtain $\mu = (231 \pm 9)\,\mathrm{cm}^2/\mathrm{Vs}$ and $(366 \pm 35)\,\mathrm{cm}^2/\mathrm{Vs}$, for 6H- and 3C-SiC, respectively, in reasonable agreement with values obtained by DC Hall measurements on doped samples at room temperature.[23,24]

Let us finally consider the relaxation of the photoinduced charge carriers. Figure 4 shows the pump-induced changes $\Delta W = \int \mathrm{d}t\, \left[E^2(t) - E_0^2(t)\right]$ in the integrated THz pulse energy as a function of the optical-pump / THz-probe delay. Note that ΔW scales with the instantaneous carrier density. For the 3C-SiC sample, the signal remains virtually constant over a time window of 800 ps, indicating a carrier lifetime on a time scale of nanoseconds or longer. In addition, we observe a quite unusual pump-fluence behavior: at high carrier concentrations, an increase of the lifetime is observed, contrary to a lifetime decrease expected from bimolecular and/or Auger recombination mechanisms.[22] Both observations are consistent with previous studies covering millisecond time windows with nanosecond time resolution.[10,11] The relaxation and recombination mechanism of photogenerated carriers in 3C-SiC is not yet well understood and requires further studies, beyond the scope of the present work.

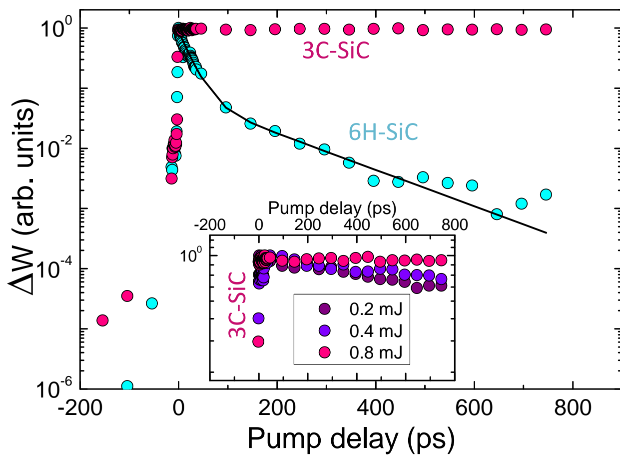

FIG. 4. Temporal decay of the pump-induced change ΔW in the THz pulse energy which scales with the density of photoinduced carriers. Carriers in 3C-SiC decay on a time scale of nanoseconds or longer, with the decay becoming even slower at increased pump fluence (see inset). In contrast, decay in 6H-SiC is fluence-independent and much faster, and a biexponential fit yields time constants of 23 ps and 144 ps.

On the contrary, in the case of 6H-SiC, we find a much faster decay of the photoinduced charge carriers. The semi-logarithmic plot of Fig. 4 reveals a biexponential dynamics (see solid lines), a faster process with a time constant of ≈ 20 ps, while a second, slower process proceeds on a time scale of 140 ps. Previous works with nanosecond time resolution report on even slower processes on time scales of 100 ns that are not covered in our ultrafast study. By varying the pump fluence, we do not observe a charge-density dependence of the relaxation dynamics. This observation suggests a unimolecular recombination mechanism, for example via defect states: the photoinduced carrier population consists of several distinct subpopulations, each obeying an exponential decay law with different decay constant[22]. Possibly, different excitation mechanisms (for instance nanosecond versus femtosecond pulses) enhance one population with respect to another.

In summary, we have determined the broadband THz conductivity of photoinduced charge carriers in two common SiC polytypes, 3C-SiC and 6H-SiC, on the picosecond time scale. The conductivity measured can adequately be described by the Drude model, and the resulting transport relaxation time of about 75 fs is found to be independent of photoinduced carrier density, thereby representing a sample-intrinsic transport parameter that allows us to estimate the carrier mobility. The carrier recombination dynamics in the 6H-SiC sample has been found to proceed on a 20-ps time scale, much faster than in 3C-SiC, yet more detailed investigation is necessary to understand the observed dynamics.

The Authors acknowledge funding from the European Union (Programme FP7-PEOPLE-2012-CIG, grant agreement N.PCIG12-8 GA-2012-326499, FOXIDUET), from MIUR (PRIN 2010-11, OXIDE) and the German Research Foundation (Grant KA 3305/2-1).

[1] N.G. Wright, A.B. Horsfall, and K. Vassilevski, Materials Today **11**, 16-21 (2008).

[2] M. Vashishath, and A.K. Chatterjee, Mj. Int. J. Sci. Tech. **2(03)**, 444-470 (2008).

[3] Fenger, SiC power materials: devices and applications, Springer (200x).

[4] G.L. Harris, Properties of Silicon Carbide. INSPEC, (1995).

[5] B.J. Baliga, Silicon Carbide Power Devices. World Scientific Press, (2006).

[6] A.L. Falk, B.B. Buckley, G. Calusine, W.F. Koehl, V.V. Dobrovitski, A. Politi, C.A. Zorman, P.X.-L. Feng and D.D. Awschalom, Nat. Comm. **4**, 1819 (2013).

[7] K. V. Emtsev *et al.*, Nat. Mater. **8**, 203 (2009).

[8] A. Galeckas, J. Linnros, M. Frischholz, K. Rottner, N. Nordell, S. Karlsson, and V. Grivickas, Materials Science and Engineering B **6162**, 239 (1999).

[9] A. Galeckas, J. Linnros, M. Frichholz, and V. Grivickas, Appl. Phys. Lett. **79**, 365 (2001).

[10] V. Grivickas, G. Manolis, K. Gulbinas, K. Jaraiunas, and M. Kato, Appl. Phys. Lett. **95**, 242110 (2009).

[11] G. Manolis, K. Jaraiunas, I.G. Galben and D. Chaussende, Mater. Sci. Forum 615617, 303 (2009).

[12] R. Ulbricht, E. Hendry, J. Shan, T.F. Heinz, and M. Bonn, Rev. of Mod. Phys. **83**, 543 (2011).

[13] Q. Wu and X.-C. Zhang, Appl. Phys. Lett. **68**, 1604 (1996); **70**, 1784 (1997); **71**, 1285 (1997).

[14] J. Lloyd-Hughes and T.-I. Jeon, J. Infr., Millim., Terahertz Waves **33**, 871 (2012) .

[15] resistivity above 2 and 30 MΩ/cm for 3C- and 6H-SiC, respectively.

[16] R.G. Humphreys, D. Bimberg and W. J. Choyke, Solid State Commun. **39**, 163 (1981).

[17] D. Olego, M. Cardona and P. Vogi, Phys. Rev. B **25**, 3878 (1982).

[18] J.H. Strait, P.A. George, J. Dawlaty, S. Shivaraman, M. Chandrashekhar, F. Rana, and M.G. Spencer, Appl. Phys. Lett. **95**, 051912 (2009).

[19] N.T. Son, C. Hallin and E. Janz'en, Phys. Rev. B **66**, 045304 (2002).

[20] J. Kono, S. Takeyama, H. Yokoi, N. Miura, M. Yamanaka, M. Shinohara and K. Ikoma, Phys. Rev. B **48**, 10909 (1993).

[21] L.V. Titova and F.A. Hegmann, Phys. in Canada, **65**, No 2, 101-104 (2009).

[22] A. Rubano, D. Paparo, F. Miletto Granozio, U. Scotti di Uccio and L. Marrucci, J. of App. Phys., **106**, 103515 (2009).

[23] S. Nishino, J.A. Powell and H.A. Will, Appl. Phys. Lett. **42**, 460-462 (1983).

[24] W.J. Schaffer, H.S. Kong, G.H. Negley and J.W. Palmour, Inst. Phys. Conf. Ser. **137**, 155 (1994).